

A Generalized Matrix Profile Framework with Support for Contextual Series Analysis

Dieter De Paepe, Sander Vanden Hautte, Bram Steenwinckel, Filip De Turck, Femke Ongenae, Olivier Janssens, Sofie Van Hoecke

IDLab, Ghent University – imec, Ghent, Belgium

Abstract

The Matrix Profile is a state-of-the-art time series analysis technique that can be used for motif discovery, anomaly detection, segmentation and others, in various domains such as healthcare, robotics, and audio. Where recent techniques use the Matrix Profile as a preprocessing or modelling step, we believe there is unexplored potential in generalizing the approach. We derived a framework that focuses on the implicit distance matrix calculation. We present this framework as the Series Distance Matrix (SDM). In this framework, distance measures (SDM-generators) and distance processors (SDM-consumers) can be freely combined, allowing for more flexibility and easier experimentation. In SDM, the Matrix Profile is but one specific configuration. We also introduce the Contextual Matrix Profile (CMP) as a new SDM-consumer capable of discovering repeating patterns. The CMP provides intuitive visualizations for data analysis and can find anomalies that are not discords. We demonstrate this using two real world cases. The CMP is the first of a wide variety of new techniques for series analysis that fits within SDM and can complement the Matrix Profile.

Keywords:

Time Series, Anomaly Detection, Matrix Profile, Distance Matrix, Series Distance Matrix, Contextual Matrix Profile

Email address: `dieter.depaepe@ugent.be` (Dieter De Paepe)

¹ **1. Introduction**

² The need for data analysis is increasing as more data is being recorded,
³ stored and made available. One driving factor is the rise of the *Internet of*
⁴ *Things* (IoT), where traditional *dumb* devices such as vehicles, household
⁵ appliances or city infrastructure are enhanced with internet connectivity for
⁶ monitoring and/or control. In 2018, there were an estimated 7 billion active
⁷ IoT devices, and this number is expected to double in about 5 years [1]. Many
⁸ sensors perform periodic monitoring, creating the need for a subdomain of
⁹ data analysis: series analysis.

¹⁰ Series analysis techniques deal with ordered collections of data points,
¹¹ rather than independent data points. Time series are most common, mea-
¹² suring specific features across time. However, not all series are time series.
¹³ For example, in [2], skull outlines in images are converted to a series for
¹⁴ classification purposes. Unlike non-series, consecutive points in series carry
¹⁵ meaning and patterns will often occur throughout the series. Finding and
¹⁶ analyzing these patterns can allow better insights in the data.

¹⁷ From a business point of view, series analysis can lead to decreased costs.
¹⁸ One such case is maintenance in industry [3]. Today, to prevent the high
¹⁹ cost of unexpected machine breakdowns, machine owners perform preven-
²⁰ tive maintenance periodically. With condition-based maintenance, sensors
²¹ monitor the health of a machine by recording and analysing time series data
²² to gain insights. This way, machine health is known and owners can better
²³ align planned maintenance with the actual need for maintenance, resulting in
²⁴ fewer interventions and decreased maintenance costs and machine downtime.
²⁵ A different business case can be made for trend prediction and anomaly de-
²⁶ tection [4]. Imagine an online service provider that monitors various metrics
²⁷ related to the usage and load of their services. If the provider is able to gain
²⁸ insight in the usage patterns of the service, he can anticipate certain trends
²⁹ and be made aware of unexpected behavioral patterns of their users. This
³⁰ not only allows the provider to allocate resources more dynamically, but also
³¹ gives him more time to act on unexpected behavior that might lead to more
³² severe issues.

³³ One state-of-the-art series analysis technique is the Matrix Profile [5], in-
³⁴ troduced by Yeh et al. in 2016. Given two series S_1 and S_2 , and a window
³⁵ length m , the Matrix Profile is a new series of length $|S_1| - m + 1$ containing
³⁶ the distance between any window of S_1 and its best matching window in
³⁷ S_2 . By itself, the Matrix Profile can be used to find the *top motifs* (the best

38 matching subsequences in a series) and the *top discords* (the most unique sub-
39 sequences in a series). Subsequently, it can be used for anomaly detection in
40 contexts where anomalies are defined by unique behavior. Since its inception,
41 many techniques have been published that either extend the Matrix Profile
42 or use it as a building block for new insights [6, 7, 8, 9, 10, 11, 12, 13, 14, 15].

43 While much progress has been made by going forward with the Matrix
44 Profile, we believe there is also value in taking a step back. One of the implicit
45 steps during the Matrix Profile calculation is the fragmented calculation of
46 the distance matrix of all subsequences of the two input series. In this paper
47 we present the Series Distance Matrix (SDM) framework as the base building
48 block on which specialized techniques can be built, rather than the Matrix
49 Profile itself. To the best of our knowledge, we are the first to present such an
50 overarching framework. Whereas several methods to calculate the distance
51 matrix have been published [5, 6, 16, 13, 14], they have never been suggested
52 as (part of) an overarching framework.

53 The presented SDM framework separates components that calculate dis-
54 tances between subsequences of input series (*SDM-generators*) and compo-
55 nents processing these distances in a meaningful way (*SDM-consumers*).
56 Existing Matrix Profile extensions from literature can be packaged as ei-
57 ther SDM-generators or SDM-consumers and plugged into the SDM frame-
58 work. By separating these components, it becomes easier to combine dif-
59 ferent techniques freely without additional effort or overhead, resulting in
60 a much broader arsenal of techniques that can be tried on new challenges.
61 Furthermore, distances can be generated once but processed by multiple con-
62 sumers in combined calculations, resulting in an overall more efficient solu-
63 tion. Lastly, because of this decoupling, components will be smaller, simpler
64 and can be optimized independently from each other.

65 We also introduce the Contextual Matrix Profile (CMP) and a new SDM-
66 consumer to calculate the CMP. The CMP can be seen as a configurable, 2-
67 dimensional version of the Matrix Profile, that tracks multiple matches across
68 window regions of the series whereas the Matrix Profile tracks one match for
69 each window. Besides data visualization, it can also be used for detecting
70 *anomalies that are not discords*. As a component of SDM, the CMP can be
71 calculated for any distance measure and can be calculated in parallel with
72 other techniques such as the Matrix Profile.

73 To summarize, our contributions in this paper are as follows: First, we
74 use a new interpretation of the distance matrix to form the generalized SDM
75 framework, which retrofits many published techniques in SDM-generators

76 or SDM-consumers. As second contribution, we introduce the Contextual
 77 Matrix Profile as a new SDM-consumer. As final contribution, we created
 78 an open source Python implementation of our SDM framework, our CMP-
 79 consumer and several Matrix Profile-based consumer and generator imple-
 80 mentations based on literature [5, 6, 10, 12, 17, 16, 15]. To the best of our
 81 knowledge, this is be the first Python library that provides an implementa-
 82 tion combining this many techniques.

83 The remainder of this paper is structured as follows: Section 2 gives an
 84 overview of literature regarding the Matrix Profile. In Section 3, we describe
 85 our SDM framework. Section 4 describes our CMP as well as the new SDM-
 86 consumer to calculte it. Its value is demonstrated for data visualization
 87 and anomaly detection for two real world datasets in Section 5. Finally, we
 88 conclude our findings in Section 6.

89 **2. Background and Related Work**

90 In this section, we formalize the definitions used in this paper, summarize
 91 the core details of the Matrix Profile and list related literature.

92 *2.1. Definitions*

93 We start by defining the common concepts of *series* and *subsequences*.

94 **Definition 1.** A series $\mathbf{S} \in \mathbb{R}^n$ is an ordered collection of n real values
 95 $(s_0, s_1 \dots s_{n-1})$.

96 **Definition 2.** A subsequence $\mathbf{S}_{i,m}$ is the continuous subsequence of \mathbf{S} start-
 97 ing at index i of length m : $(s_i, s_{i+1} \dots s_{i+m-1})$. The subsequence cannot be
 98 longer than the original series ($1 \leq m \leq n$) and has to fall completely within
 99 \mathbf{S} : $(0 \leq i \leq n - m)$.

100 The distance measure used in the Matrix Profile is the *z-normalised Eu-*
 101 *clidean distance*. The reason for this is explained in the next subsection.

102 **Definition 3.** The z-normalised series $\hat{\mathbf{S}}$ is constructed by transforming \mathbf{S}
 103 so it has a mean $\mu = 0$ and standard deviation $\sigma = 1$: $\hat{\mathbf{S}} = \frac{\mathbf{S} - \mu_S}{\sigma_S}$.

104 **Definition 4.** The z-normalised Euclidean distance $D_{ZE}(\mathbf{A}, \mathbf{B})$ between 2
 105 series of equal length $A \in \mathbb{R}^m$ and $B \in \mathbb{R}^m$ is defined as the Euclidean
 106 distance D_E of the z-normalised series $\hat{\mathbf{A}}$ and $\hat{\mathbf{B}}$.

$$D_{ZE}(\mathbf{A}, \mathbf{B}) = D_E(\hat{\mathbf{A}}, \hat{\mathbf{B}}) = \sqrt{(\hat{a}_0 - \hat{b}_0)^2 + \dots + (\hat{a}_{m-1} - \hat{b}_{m-1})^2}$$

107 2.2. Matrix Profile

108 In 2016, Yeh et al. [5] published a novel technique to perform *series subsequence all-pairs-similarity-search* on two series, producing two new series:
109 the Matrix Profile and the Matrix Profile Index. The Matrix Profile is defined
110 as the vector containing the z-normalized Euclidean distances between each
111 subsequence from the first series and its closest matching subsequence from
112 the second time series. The Matrix Profile Index contains the subsequence
113 index in the second series for each match.

114 Concretely, given two series $\mathbf{S1} \in \mathbb{R}^n$ and $\mathbf{S2} \in \mathbb{R}^k$ and a subsequence
115 length m , the Matrix Profile $\mathbf{M} \in \mathbb{R}^{n-m+1}$ and Matrix Profile Index $\mathbf{I} \in$
116 \mathbb{R}^{n-m+1} are new series such that for each $i \in [0, n - m]$, \mathbf{I}_i contains the index
117 of the start of the subsequence of $\mathbf{S2}$ of length m that best matches $\mathbf{S1}_{i,m}$ and
118 \mathbf{M}_i contains the corresponding distance. In the case a *self-join* is performed
119 where $\mathbf{S1} = \mathbf{S2}$, an additional constraint is added to prevent *trivial matches*,
120 where subsequences match themselves or nearby subsequences.

121 The default distance measure used is the z-normalized Euclidean distance,
122 which has been shown [18] to provide better results by removing the effect of
123 a changing data offset over time and thus focussing more on shape instead
124 of amplitude. Typical causes of a changing offset are wandering baselines
125 in sensors or natural phenomena (e.g., the gradual change in temperature
126 throughout seasons).

128 2.3. Related Work

129 Literature related to the Matrix Profile can be separated into 3 cate-
130 gories: related work focusing on a) the calculation of the Matrix Profile, b)
131 techniques that gain insights from the Matrix Profile or the Matrix Profile
132 Index, and finally, c) ideas from the Matrix Profile for tackling new problems.

133 **a) Calculation of the Matrix Profile**

134 The Matrix Profile was published together with the STAMP algorithm [5], an
135 anytime algorithm to calculate the Matrix Profile (and corresponding Index)
136 of a series of length n in $O(n^2 \log n)$ time. STAMP uses the MASS algorithm
137 [19] to iteratively calculate the distances for each subsequence. Performance
138 was later improved by the STOMP algorithm [6], which uses a dynamic pro-
139 gramming technique to reduce the runtime to $O(n^2)$, at the cost of losing
140 the anytime property. Another optimization came with the SCRIMP algo-
141 rithm [16], which restores the anytime property while retaining the same
142 complexity as STOMP. Finally, ACAMP provides another speed improve-
143 ment by postponing some operations until the Matrix Profile is completed

[13]. We extended the calculation to reduce the effects of noise when dealing with flat sequences [15, 20], others have made extensions for handling missing data points [21] and support for calculating the multidimensional Matrix Profile [10].

Several recent works have suggested different distance measures to be used in the Matrix Profile. Silva et al. [22] use the Matrix Profile with the (non-normalized) Euclidean distance to perform music recognition and thumbnailing. Akbarinia et al. [13] suggest that using the Euclidean distance, and more general p-norm might be more useful for data analysis in physics, statistics, finances and engineering. Though they present no evaluations, one can expect relevant results for cases where series are not subjected to wandering baselines [18], such as system monitoring. Another distance measure suggested is ψ -DTW [14]. The authors claim that for many application domains, the z-normalized Euclidean distance is too strict while looking for motifs and discords. The ψ -DTW measure performs a non-linear transformation along the (time) axis and can ignore a prefix or suffix of the subsequence being matched. The authors find improved results for domains such as motion tracking (e.g., athlete positioning, motion capture and gesture analysis) and music data mining, though they underline the difficulty of objectively evaluating the relevance of motifs and discords.

b) Gaining insights

Insight in a series can be gained using the Matrix Profile (Index). Motif and discord discovery consist of finding the top matching and worst matching subsequences in a series and can be solved quickly by finding the minima and maxima in the Matrix Profile [5]. Discord discovery can be interpreted as a form of anomaly detection (which has a wide range of applications in machine maintenance, healthcare or system monitoring). In cases where the user knows the type of pattern they are looking for, they can use the Annotation Vector [9] to transform the Matrix Profile before performing motif/discord discovery. Other insights are also possible such as finding gradually changing patterns [11] or finding changes in the underlying behavior being measured [12, 15].

c) Matrix Profile as a building block

The series motifs found by the Matrix Profile have been used for data visualization [7] and classification [8] techniques. Furthermore, a series summarization technique [23] has been published which uses *MPDist*, a distance measure that considers two sequences similar if they share many similar subsequences [24]. The calculation of MPDist involves finding the best match for

182 all subsequences in both series. These could be found by performing a double
183 Matrix Profile calculation, but can also be obtained in a single calculation
184 by processing the subsequence distances in a different way.

185 As we can see, a wide range of techniques has emerged, most focusing on
186 an aspect closely related to the Matrix Profile.

187 3. The Series Distance Matrix

188 Many of the works in Section 2 have started from the idea of the Matrix
189 Profile and created a new algorithm to obtain one specific variation. Looking
190 forward to the future, we can expect the amount of algorithms to rise
191 dramatically as the different distance measures and processing methods are
192 further expanded and combined. Instead, we propose to view these variations
193 as instances of a more generalized framework which we call the *Series
194 Distance Matrix* (SDM).

195 3.1. SDM: General Concept

196 We present SDM as a component based framework for deriving insights
197 by processing pairwise distances of the subsequences of pairs of series (this
198 includes self-joins by assuming two equal series). Given pairs of series, *SDM-
199 generators* are responsible for calculating the distances between all pairs of
200 subsequences. Because calculating the full distance matrix is not scalable,
201 we instead calculate fragments of the distance matrix. These fragments are
202 processed by the *SDM-consumers*, after which the fragment is discarded and
203 a new fragment is calculated. Each consumer is responsible for processing
204 all distance fragments in a way that provides certain insights.

205 Conceptually, the distance matrix fragments can take any form, however,
206 columns and diagonals have proven to work well for the Matrix Profile. The
207 column based approach is used by the STOMP algorithm [6], it has the
208 advantage of being easier to implement and is more suited for cases where
209 one series is being streamed in an online fashion, since each new data point
210 results in one new column of distance matrix values. The diagonal approach
211 is used by the SCRIMP [16] algorithm. By processing diagonal fragments
212 of the distance matrix, the calculated distances of each fragment are spread
213 over many different pairs of subsequences. This can be utilised by some
214 consumers, such as the Matrix Profile, to provide approximate intermediate
215 results when processing all data takes a long time, making it well suited for
216 interactive use cases.

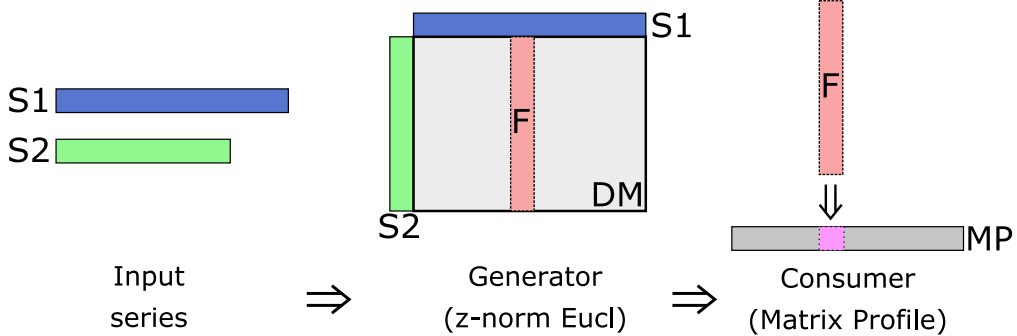


Figure 1: The Matrix Profile calculation fitted into the SDM framework. Starting from two input series (S_1, S_2), the z-normalized Euclidean distance generator iteratively creates fragments, in this case columns (F), of the distance matrix of all subsequences (DM). Each of these fragments are processed by the Matrix Profile consumer, storing the minimum value for each column in the resulting Matrix Profile (MP).

217 Figure 1 shows a schematic visualization of the Matrix Profile calculation
 218 fitted into the SDM framework.

219 By separating the distance calculation and processing, we can easily com-
 220 bine generators and consumers to our needs. For example, the techniques de-
 221 scribed by Akbarinia et al. [13] and Furtado Silva et al. [14] are a combina-
 222 tion of the p-norm or ψ -DTW generator with a Matrix Profile consumer. Com-
 223 binations that have not yet been researched, such as combining a ψ -DTW
 224 generator with an MPDist consumer, are - thanks to the SDM framework -
 225 just as straightforward. A second benefit is that multiple consumers can be
 226 configured for a single generator, instead of having to adjust the algorithms
 227 itself, this way reducing calculation overhead. Lastly, by adopting a com-
 228 ponent based design, each component can be optimized independent of the
 229 others. For example, if a faster way is found to calculate the z-normalized
 230 Euclidean distance, only one generator has to be updated, instead of every
 231 technique using the z-normalized Euclidean distance.

232 3.2. *SDM: Python Implementation*

233 As part of this paper, we released a Python library¹ under the MIT
 234 license implementing our SDM framework and CMP consumer. In addition

¹<https://github.com/IDLabResearch/seriesdistancematrix/>

235 to the contributions of this paper, it contains implementations for the noise-
236 corrected z-normalized Euclidean distance ([5, 6, 16, 15]), Euclidean distance,
237 Matrix Profile [5], Multidimensional Matrix Profile [10], Left- and Right-
238 Matrix Profile [11] and VALMOD [17]. It supports batch operations as well
239 as streaming data. At the time of writing, and to the best of our knowledge,
240 this is the first public Python library integrating this many different Matrix
241 Profile related work as consumers and generators in our generic framework.

242 4. Contextual Matrix Profile

243 This section covers a new series analysis technique, the CMP, which can
244 easily find repeated patterns in series and shares the benefits of the Ma-
245 trix Profile: it is deterministic, domain agnostic, exact and is suited for
246 parallelization. The CMP is calculated by the CMP-consumer in the SDM
247 framework. Note that thanks to the SDM framework, we can focus purely on
248 how the calculated distances should be processed, since we can combine the
249 CMP with *any distance measure* that has a corresponding SDM-generator
250 implementation.

251 As the name implies, the CMP is closely related to the Matrix Profile,
252 and can be best explained in how it differs from it. We make our compari-
253 son starting from the distance matrix (the implicit matrix containing the
254 distances of all subsequences from the first input series to all subsequences
255 from the second input series). Where the Matrix Profile is defined as the
256 column-wise minimum over the entire distance matrix, the CMP is defined
257 as the minimum over rectangular regions of the distance matrix. These rect-
258 angles may overlap and may or may not cover the entire distance matrix.
259 Their configuration is up to the user. A visual comparison of the Matrix
260 Profile and the CMP can be seen in Figure 2. Note that the CMP-consumer
261 may be configured in such a way that it calculates the Matrix Profile. In this
262 way, the CMP can be seen as a generalization of the Matrix Profile.

263 Given two input series S_1 and S_2 and subsequence length m , the Matrix
264 Profile looks for the best matching subsequence in S_2 for any subsequence in
265 S_1 . The CMP on the other hand looks for the best matching subsequence
266 in ranges over S_1 and S_2 . These ranges allow us to group the data in dif-
267 ferent ways and can reveal new insightful patterns. Specifically, because we
268 aggregate the distances in ranges across both series, the CMP is very good at
269 picking up repeated patterns, even if these patterns are not strictly periodic.

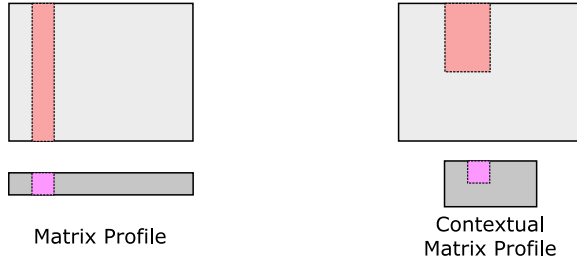


Figure 2: Matrix Profile and CMP differ in how they are created using the distance matrix (light gray). The Matrix Profile (dark gray, left) consists of the column-wise minimum of the values in the distance matrix. The Contextual Matrix Profile (dark gray, right) is created by taking the minimum over rectangular areas. Note that these areas may overlap and may or may not cover the entire distance matrix, depending on the user configuration.

270 We will show two use cases for the CMP, i.e., data visualization and anomaly
271 detection, but first we discuss more thoroughly how the CMP is calculated.

272 *4.1. Calculating the CMP*

273 Many specialized algorithms could be conceived for specific region config-
274 urations. Here, we provide a general purpose algorithm. In this algorithm,
275 the regions of interest are provided by specifying ranges along the dimen-
276 sions of the distance matrix. This principle is illustrated in Figure 3. One
277 advantage of this approach is that for non-overlapping ranges, the resulting
278 CMP resembles a reduced distance matrix. We will exploit this property in
279 our use cases below.

280 Our algorithm assumes the distance matrix is provided in a column-wise
281 manner (similar to the STOMP algorithm [6]). A straightforward adaptation
282 for diagonals is also made available in our reference implementation.

283 The initialization of the CMP-consumer is outlined in Algorithm 1. We
284 take two lists of ranges as input, each defining the contexts for one of the
285 input series. We store the ranges in line 1 and 2. Next, we prepare containers
286 for the CMP and corresponding indices, similar to the Matrix Profile Index.
287 Note that the CMP indices are two-dimensional since we need to track the
288 exact match index for both input series.

289 The actual calculation of the CMP is listed in Algorithm 2. In line 1, we
290 iterate over all ranges defined over the horizontal dimension of the distance
291 matrix and skip any that do not contain the column being processed in lines
292 2-4. Next, we iterate over all ranges for the vertical axis. Since all ranges will

Algorithm 1: CMP-consumer Initialization

Input : $R1$, ranges for the vertical axis of the distance matrix. A range is a pair defining a start (inclusive) and end (exclusive) index.

Input : $R2$, ranges for the horizontal axis of the distance matrix.

```

1 v_ranges  $\leftarrow R1$ ;
2 h_ranges  $\leftarrow R2$ ;
3 cmp  $\leftarrow |R1| \times |R2|$  matrix, filled with  $+\infty$ ;
4 cmp_index  $\leftarrow |R1| \times |R2|$  matrix, filled with  $(-1, -1)$ ;
```

Algorithm 2: CMP-consumer Column Processing

Input : The column index col .

Input : A vector d containing all distances on column col .

```

1 for  $j, h\_range \leftarrow \text{enumerate}(h\_ranges)$  do
2   if  $col$  not in  $h\_range$  then
3     continue
4   end
5   for  $i, v\_range \leftarrow \text{enumerate}(v\_ranges)$  do
6      $dists \leftarrow d[v\_range]$ ;
7      $min\_dist \leftarrow \min(dists)$ ;
8     if  $min\_dist < cmp[i, j]$  then
9        $cmp[i, j] \leftarrow min\_dist$ ;
10       $row \leftarrow \text{argmin}(dists) + v\_range[0]$ ;
11       $cmp\_index[i, j] \leftarrow (row, col)$ ;
12    end
13  end
14 end
```

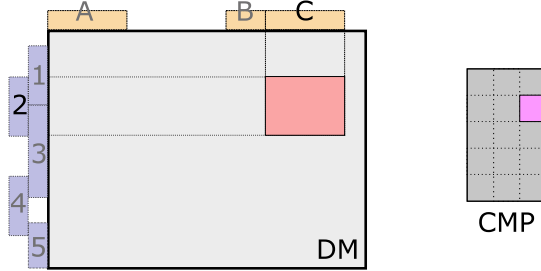


Figure 3: Example of region definitions: a user has specified three horizontal ranges (A, B, C) and five vertical ranges (1...5) on the axes of the distance matrix (DM). Any pair of ranges from both axes corresponds to one region of interest in the distance matrix. The minimum value of the region is calculated and stored in the CMP. Note that the ranges may overlap and may or may not fully cover the distance matrix dimensions.

293 have some overlap with the distance matrix column, we do not need to filter.
 294 In lines 6 and 7, we determine the minimum value of the distance matrix
 295 column that is contained in both ranges. We compare this minimum against
 296 the best value so far and update the distance and corresponding index if we
 297 find a better match (lines 8-12).

298 Note that when h_ranges is very long, a linear scan becomes inefficient.
 299 Depending on the intended use, optimizations are obvious: tree maps for
 300 general cases, hash based lookup for strictly periodic ranges, or storing the
 301 search index for non-overlapping ordered ranges. In this section, we did not
 302 attempt to list all possibilities and instead presented the approach best suited
 303 for understanding the technique.

304 Lastly, we briefly discuss the complexity of the CMP. Strictly speaking,
 305 the space complexity is constant as it is determined by the configuration of
 306 the vertical (V) and horizontal (H) ranges: $O(|H||V|)$. When ranges will
 307 be defined in function of the length of the input series (n), $O(n^2)$ is more
 308 representative. Note that this last form is overly pessimistic as $|H|$ and $|V|$
 309 will typically be much smaller than n . The time complexity for *processing*
 310 *a single column* is $O(|H| + |V| \times S)$, where S represents the average span
 311 of a vertical range. In a typical case where ranges will not overlap, this can
 312 be simplified to $O(n)$. As such, a full calculation can be done in $O(n^2)$, the
 313 same complexity as the calculation of the Matrix Profile using STOMP.

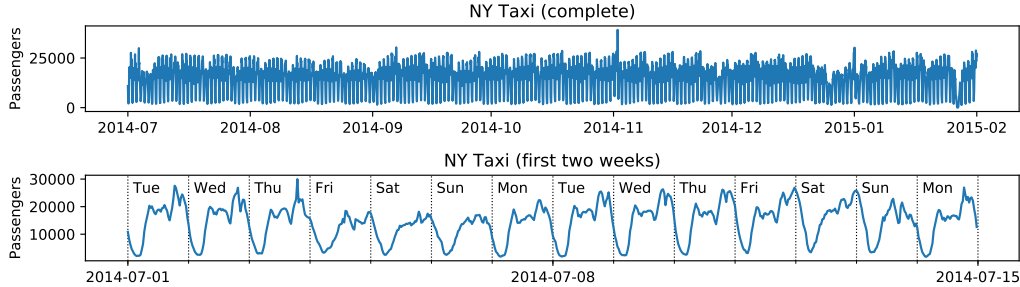


Figure 4: The New York Taxi dataset from the Numenta Anomaly Benchmark. It lists the summed number of taxi passengers in New York at 30 minute intervals. Top: Complete dataset. Bottom: The first two weeks of the dataset, where we see a clear periodic pattern. Note how the pattern for the first Friday, Independence Day, resembles the pattern for a weekend day.

314 5. CMP for Data Visualization and Anomaly Detection

315 We will demonstrate the value of the CMP using two different use cases:
 316 data visualization and anomaly detection. For both cases, we use the public
 317 New York Taxi dataset and a dataset delivered to us by Renson (a ventilation
 318 manufacturing company) that we share as part of this publication [25].
 319 Additionally, in our most recent paper [20], we combine the CMP with the
 320 noise elimination technique [15] to visualize a UCI activity dataset and show
 321 potential for activity segmentation as well. Note that it is not our goal to im-
 322 prove upon the state-of-the-art anomaly detection techniques in this section,
 323 but rather to show the potential of the CMP.

324 All figures in this section were created using Python-based Jupyter note-
 325 books, which we have shared online [25]. Besides providing an easy way to
 326 reproduce our results, they offer some additional visualizations we omitted
 327 due to size constraints.

328 5.1. New York Taxi Dataset: Data Visualization

329 The first dataset is the New York Taxi public dataset from the Numenta
 330 Anomaly Benchmark [26]. It lists the total number of taxi passengers in New
 331 York city for a period from July 2014 up to February 2015, bucketed per half
 332 hour. An overview and excerpt is shown in Figure 4.

333 We calculated the CMP by self-joining the data using the z-normalized
 334 Euclidean distance, using a window length of 44 (22 hours) and a daily

335 context starting at midnight until 02:00 in the morning. Because we are self-
336 joining the data, a constraint prevents any day from matching itself. Simply
337 put, we are asking for the most (shape-wise) similar subsequences between
338 any pair of days, where either subsequence is 22 hours long and can start
339 between midnight and 02:00. These values were based on a quick visual
340 inspection of the data. By choosing a two hour context range and a 22 hour
341 window length, we allow temporal shifts when comparing windows, while
342 always comparing values of the same day. Note that for slightly different
343 values, we obtained similar results. Since the dataset contains 215 days and
344 we define one context per day, the resulting CMP is a 215 by 215 matrix.
345 It is shown in Figure 5. Note that the CMP is symmetrical because of the
346 self-join, higher values in the CMP correspond to more dissimilarity.

347 When visualized, the CMP can be used to gain insight into the dataset
348 it was built on. For example, the pattern of small squares visible in Figure 5
349 indicates that there are typically 5 days displaying similar behavior, followed
350 by 2 days of different behavior. These patterns are of course caused by
351 the cycle of weekdays and weekends. Other artefacts standing out are the
352 wide band around New Year, near the end of November (Thanksgiving) and
353 the stripe near the end of January (when a blizzard struck New York), all
354 indicating different behavior in the dataset.

355 Visualizations like these help data scientists explore new datasets. By in-
356 specting the CMP, they can find patterns and deviations from these patterns
357 that might require further investigation (as we will do in our next use case).
358 Another application is the creation of visual thumbnails for series, helping
359 users to navigate large collections of series. Other thumbnail techniques have
360 been presented using SAX [27] and time series snippets [23] but are unable
361 to provide this degree of insight into the underlying patterns.

362 Of course, the Matrix Profile can also be visualized to gain insight in
363 a series. We calculated the Matrix Profile using the same parameters as
364 the CMP, it is shown in Figure 6. As mentioned before, the Matrix Profile
365 is a one dimensional vector where high values correspond to more unique
366 subsequences. Looking at the figure, we gain some insights in where the data
367 displays unique behavior, which is further explored in Section 5.2. However,
368 the Matrix Profile is unable to capture the periodic nature of the data since
369 each sequence is compared against all other sequences rather than multiple
370 spans like the CMP does.

371 As a final demonstration of the possibility to gain insights from visual-
372 izing the CMP, we would like to share an unexpected trivia we discovered.

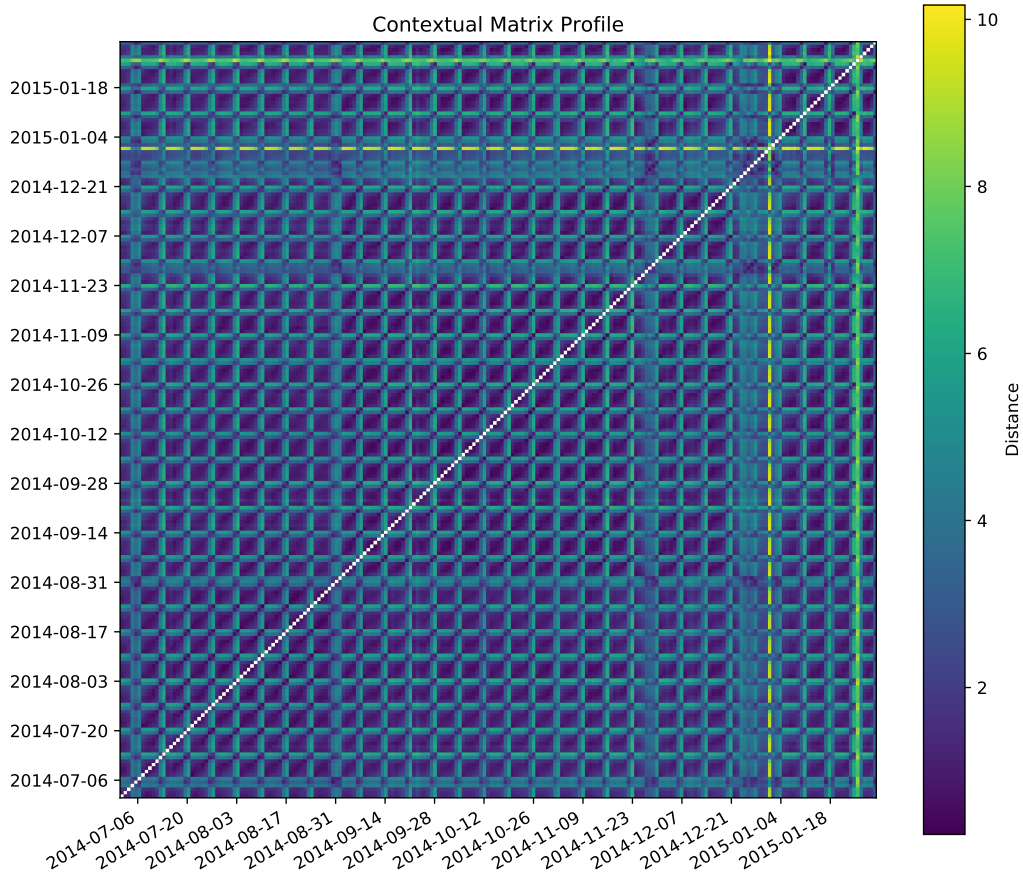


Figure 5: The CMP for the New York Taxi dataset. Each point displays the distance between 2 days, defined as the z-normalized Euclidean distance between the best matching 22 hour long subsequences of both days. Lower distances correspond to a better match. We can clearly see a periodic pattern caused by weekdays versus weekends and the changed behavior around Thanksgiving and between Christmas and New Year. The bright line near the end of January is the effect of a blizzard hitting New York.

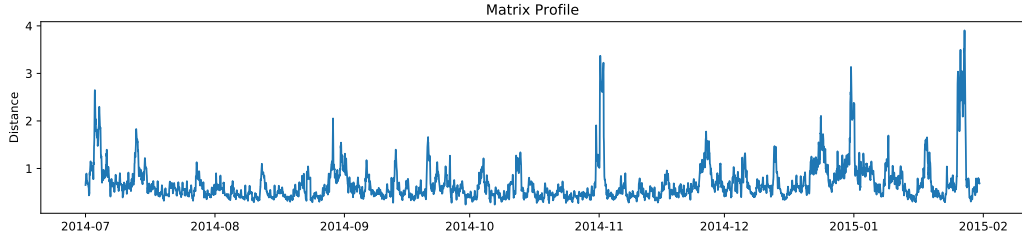


Figure 6: The Matrix Profile for the New York Taxi dataset. Each value represents the distance from the subsequence of the series starting at that index to its nearest match, where higher distances mean more unique subsequences. While we see higher values corresponding to some holidays or other events (discussed in Section 5.2), the periodic nature of the data is not captured in this visualization.

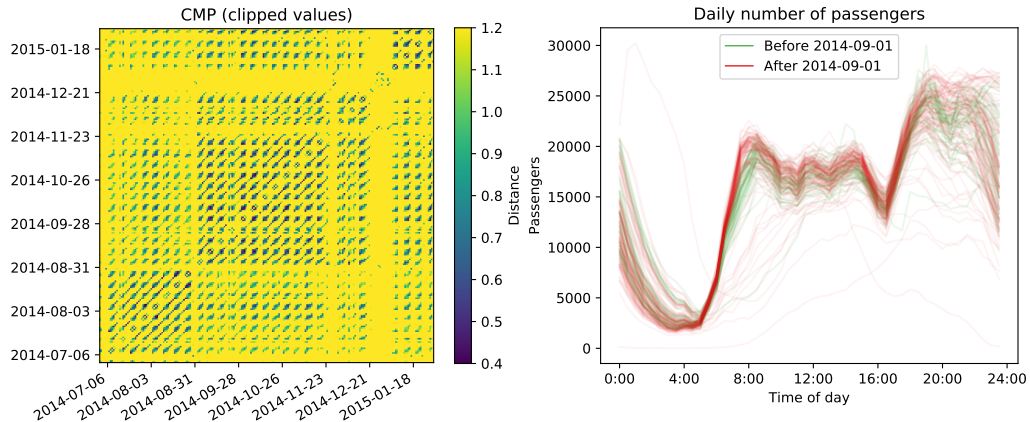


Figure 7: Left: The CMP for the New York Taxi dataset, with values restricted to the range [0.4, 1.2], highlighting the change in distance for days before and after September 1st. Right: The origin of the difference in distances. The number of taxi passengers before and after September 1st differs noticeably around 07:30 in the morning.

373 Looking carefully, one can see a small difference in the values before and
 374 after September 1st (Labor Day). This is more clearly presented in Figure
 375 7 (left). We see the days before Labor Day have a worse match with the
 376 days after Labor Day and vice versa, indicating the taxi passenger behav-
 377 ior has changed. Indeed, when looking at the daily graphs (Figure 7 right),
 378 we see a noticeable difference in the behavior around 07:30 in the morning:
 379 after Labor Day, the number of taxi passengers is higher. The most likely
 380 explanation is the start of the school year, which also falls on September 1,
 381 enabling parents to leave earlier for work.

382 5.2. New York Taxi Dataset: Anomaly Detection

383 As anomalies are defined as *patterns that do not conform to expected behavior* [28], objectively evaluating them is particularly difficult for realistic
384 datasets. What is interpreted as anomalous for one user, might be normal behavior for another [29]. While the New York Taxi dataset contains
385 a ground truth of 5 anomalies (listed in Table 1) that were specified by the
386 dataset provider as “anomalies with known causes”², we argue several deviations
387 from expected patterns are present in the data but were not included in the
388 ground truth because of background knowledge not present in the data.
389 As a result, we find the ground truth to be biased towards techniques that
390 find unique behavior, rather than unexpected behavior. Luckily, it is easy to
391 further investigate and validate suspected anomalies, as we will do next.

394 The visualization of the CMP in Figure 5 already gives a good visual
395 indication about anomalies: on some days the *expected* repetitive pattern is
396 not present. Based on the visual pattern, we divided the contexts into three
397 groups and form smaller CMPs: one containing weekdays and two containing
398 only Saturdays and only Sundays respectively. This is visualised in Figure
399 8. These reduced CMPs each represent a collection of days that we expect
400 to behave in a similar manner. Since each value in a column (or row) in the
401 CMPs indicates how much a single day (context) deviates from other days
402 (contexts), we can average each column to obtain a single value indicating
403 how much this day deviates from the other days. We define this value as the
404 anomaly score for that day. Note that we average the values in the reduced
405 CMPs, meaning that, e.g. the anomaly score of any Sunday is based on
406 how much it differs from all other Sundays in the dataset, irrespective of the
407 differences with Saturdays or weekdays. After calculating the anomaly score
408 for every day, we ordered all anomaly scores and using the Elbow method,
409 we determined a threshold to obtain 18 anomalous days in total (Figure 8
410 right). The anomalies are listed in Table 1 and visualized in Figure 9.

411 We compare the anomalies against those found by the Matrix Profile. The
412 Matrix Profile can be used to find series discords, subsequences that maxi-
413 mally differ from any other subsequence, these discords can be interpreted as
414 anomalies [5]. We calculated the anomalies using the Matrix Profile with a
415 window length of 22 hours (similar as the CMP) and not allowing overlapping
416 anomalies. We obtained 16 anomalies using the Elbow method, which are

²<https://github.com/numamenta/NAB/wiki/FAQ>

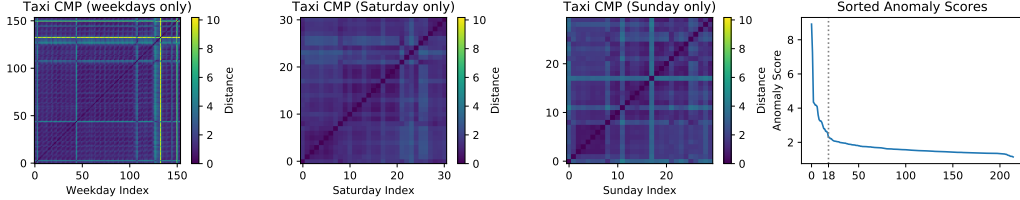


Figure 8: Reduced CMPs from Figure 5, containing only the entries for weekdays (first), Saturdays (second) or Sundays (third) on both axes. Fourth: The anomaly scores (obtained by averaging each column of all reduced CMPs), ordered from high to low. We determined the number of worthy anomalies to be 18.

417 listed in Table 1 and visualized in Figure 10. Note that the anomalies here
 418 have no starting time restriction and can partially cover one or two days.

419 Of the 25 different anomalies listed in Table 1, only nine are flagged as
 420 anomalous by both techniques. For each of these nine, a reasonable expla-
 421 nation could be found, falling into the categories of holiday (Independence
 422 Day, Thanksgiving, Martin Luther King Day), holiday predecessor (day be-
 423 fore Christmas, New Year’s Eve) or large scale event (Climate March, Day-
 424 light Savings Time and blizzard). The CMP additionally detected Labor
 425 Day, and many weekdays in the Christmas and New Years period, typical
 426 days when people take time off from work. Note that since the anomalies
 427 by the Matrix Profile can span two days, it would not be fair to consider
 428 Christmas and New Year to be found exclusively by the CMP. For one CMP
 429 anomaly no clear explanation could be found, though we suspect it is an
 430 after effect of the Independence Day celebrations. The Matrix Profile on the
 431 other hand exclusively found one weather event, one large scale event (the
 432 Millions March against police brutality), Halloween (most likely due to the
 433 effect of late-night parties) and four days for which no clear-cut explanation
 434 could be found. However, two of the unknown anomalies precede Labor Day,
 435 so this could again be an effect caused by people heading out of town for
 436 celebrations. Perhaps surprisingly, the Matrix Profile cannot detect Labor
 437 Day itself, this is because it closely matches Martin Luther King Day and two
 438 weekends in the dataset, meaning it will not be flagged as a series discord.

439 Rather than looking at individual anomalies, we can also look at the
 440 broader picture. By comparing each CMP anomaly against other days of the
 441 same type (the second or third column in Figure 9, whichever contains a solid
 442 red line), we see that all anomalous days noticeably differ from the majority
 443 of the reference days (gray band in the figure). This is less the case for the

Date	Event	Numenta	MP	CMP
Thu 2014-07-03	Evening thunderstorms		5	
Fri 2014-07-04	Independence Day		6	5
Sun 2014-07-06	<i>Unknown</i>			15
Sun 2014-07-13	<i>Unknown</i>		10	
Fri 2014-08-29	<i>Unknown</i>		8	
Sun 2014-08-31	<i>Unknown</i>		15	
Mon 2014-09-01	Labor Day			6
Sun 2014-09-21	Climate March		13	17
Fri 2014-10-31	Halloween		9	
Sun 2014-11-02	Daylight Savings Time	x*	3*	9
Thu 2014-11-27	Thanksgiving	x	11*	12
Fri 2014-11-28	Day after Thanksgiving			11
Sat 2014-12-13	Millions March		16	
Wed 2014-12-24	Christmas period		7	3
Thu 2014-12-25	Christmas	x		7
Fri 2014-12-26	Christmas period			10
Mon 2014-12-29	New Year period			14
Tue 2014-12-30	New Year period			18
Wed 2014-12-31	New Year's Eve		4	16
Thu 2015-01-01	New Year	x		1
Fri 2015-01-02	New Year period			13
Fri 2015-01-09	<i>Unknown</i>		12	
Mon 2015-01-19	Martin Luther King Day		14*	8
Mon 2015-01-26	Blizzard		2	2
Tue 2015-01-27	Blizzard	x	1	4

Table 1: Anomalies as found by the Matrix Profile (MP) and CMP as well as the ground truth for the dataset (Numenta). The numbers in column CMP and MP correspond to the ordering used in Figure 9 and 10 respectively, where a lower number indicates a higher anomalous behavior.

*: Actually listed on the preceding day, but visual inspection shows the aberrant behavior takes place after midnight.

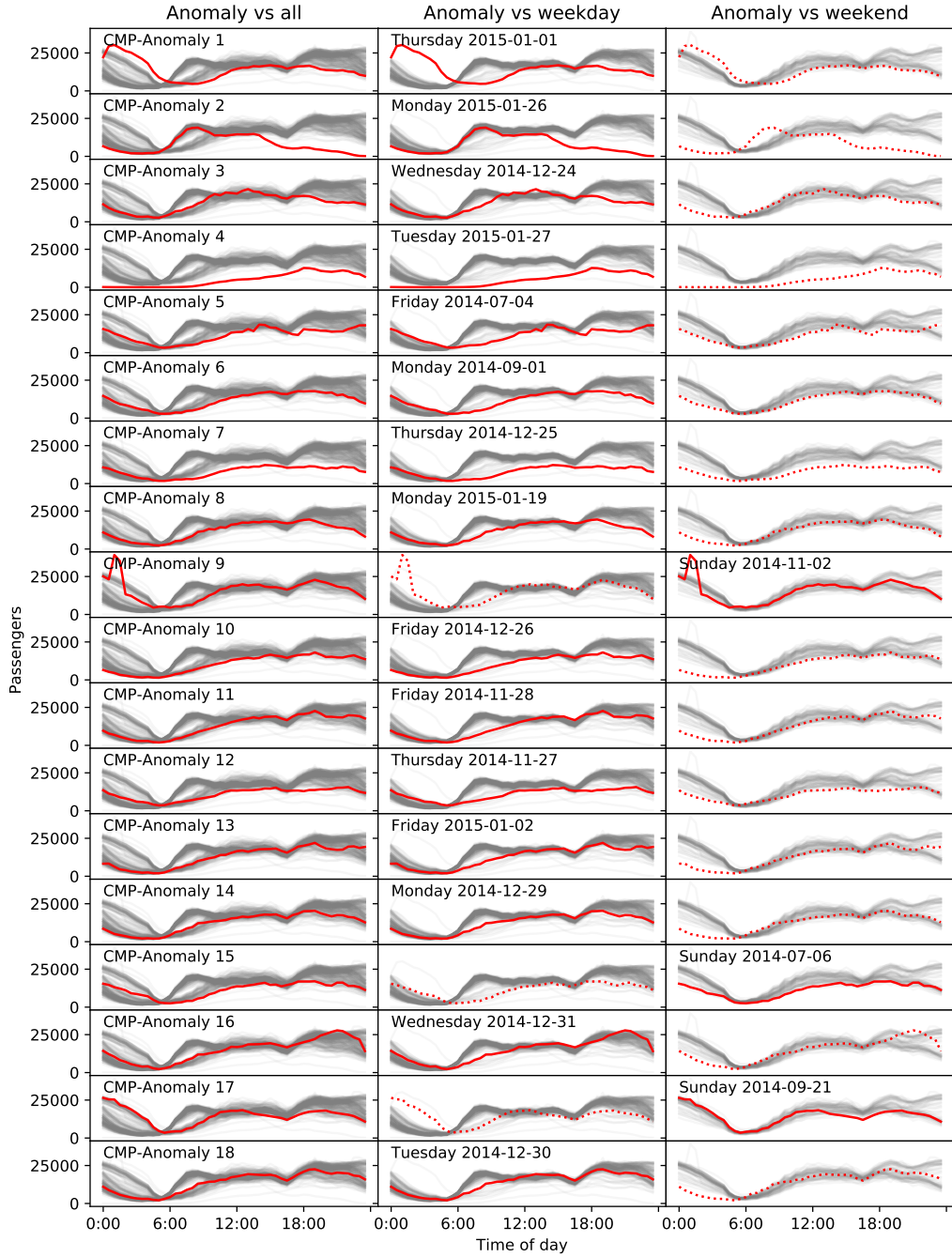


Figure 9: The 18 anomalous days found using the CMP, ordered from most anomalous to least anomalous. Each row shows one anomalous day (red) against all other days in the dataset (gray). A dotted red line is used to visualize the anomaly in the column that does not match its own type (weekday/weekend).

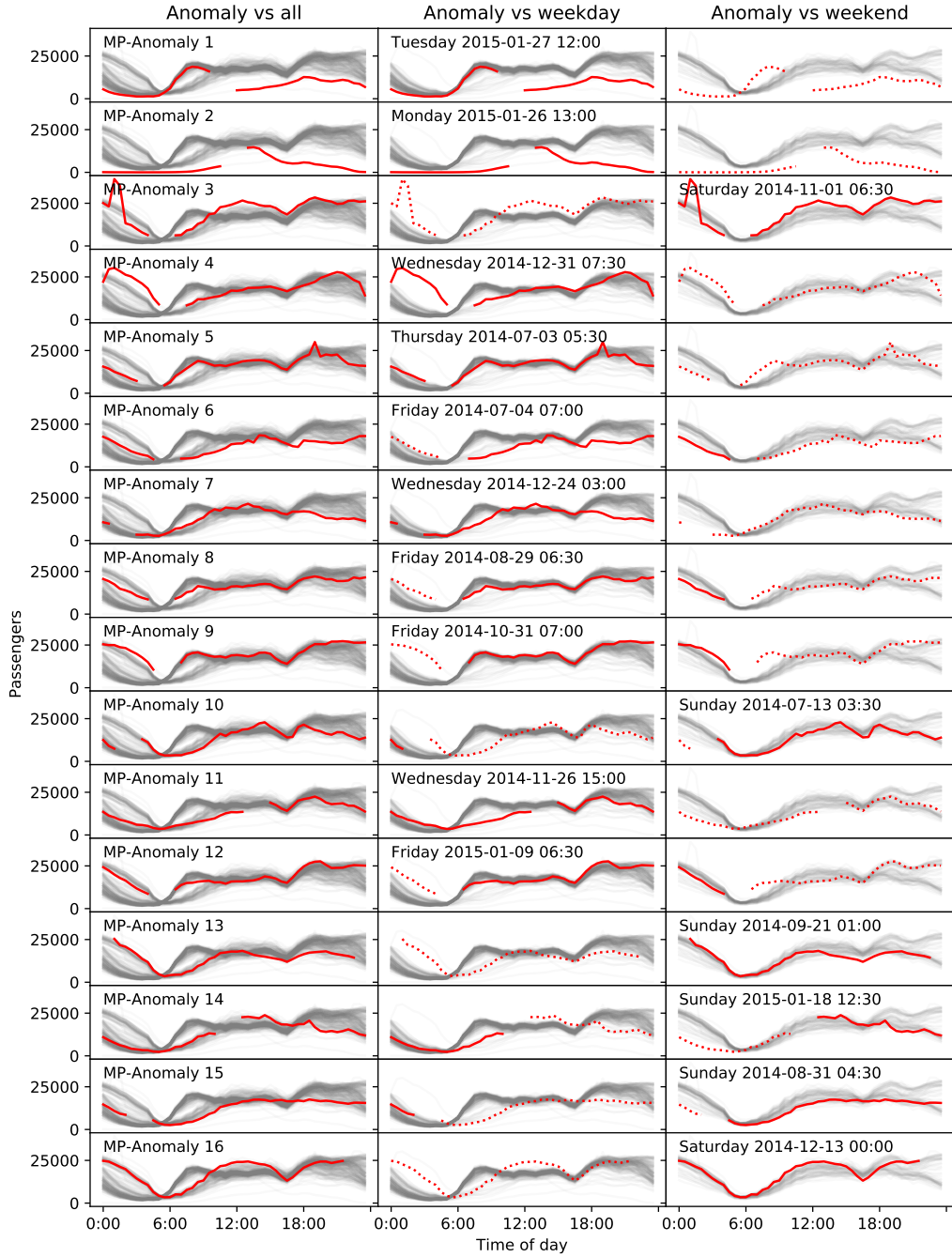


Figure 10: The 16 anomalous sequences found using the Matrix Profile, ordered from most anomalous to least anomalous. Each row shows one anomalous sequence of 22 hours (red) against all other days in the dataset (gray). A dotted red line is used to visualize the anomaly in the column that does not match its own type (weekday/weekend).

444 anomalies found by the Matrix Profile (Figure 10). Here, about half of the
445 anomalies resemble the reference days, but contain some local variation such
446 as a spike, elongated tail or less pronounced bumps.

447 The question arises: which of these techniques is best suited for anomaly
448 detection? While we suspect most users will find the results of the CMP to
449 be more insightful for this specific dataset, the general answer remains “*it*
450 *depends*”. Fundamentally, both techniques are searching for different things.
451 While the Matrix Profile is looking for the most unique patterns (discords)
452 in the series, the CMP based anomaly detection is looking for patterns that
453 differ most from a group of reference contexts. Both approaches will have
454 applications depending on the type of anomalies the user is interested in.

455 Whereas a simple distance matrix between weekdays and weekends could
456 also have found these anomalies, this assumes knowing the underlying pattern
457 in advance. One benefit of the CMP is that it allows us to discover these
458 patterns in advance when the pattern is *unknown in advance*, which is often
459 the case. So, assuming we did not know the weekday/weekend similarity
460 beforehand, we could have easily deduced it by visualizing the CMP. The
461 CMP has one other major advantage over a basic distance matrix, it allows
462 for a (time) shift when comparing sequences (for which the added value is
463 better demonstrated for the next dataset). A similar approach with typical
464 techniques would result in a high complexity, instead we can rely on the
465 computationally efficient implementations of the distance generators of the
466 SDM framework [6, 16].

467 *5.3. Ventilation Dataset: Data Visualization*

468 Our second dataset is a proprietary dataset delivered to us by Renson, a
469 ventilation manufacturing company. It contains measurements of various air
470 quality metrics such as temperature, humidity, carbon dioxide and volatile
471 organic compounds, for all rooms within a building that are connected to
472 a ventilation unit, for several anonymized buildings. The users of Renson
473 ventilation products can use this data to observe the functioning of the ven-
474 tilation system and to estimate the air quality of their home. The metrics
475 are measured at 15 minute intervals and differ per room type. Here, we focus
476 on the CO₂ sensor of rooms designated as kitchen. The dataset is shown in
477 Figure 11. Unlike the Taxi dataset, each household has a wide range of dis-
478 tinct daily behaviors and no immediate obvious repeating patterns, it is also
479 not possible to verify any root causes of anomalies. This use case represents

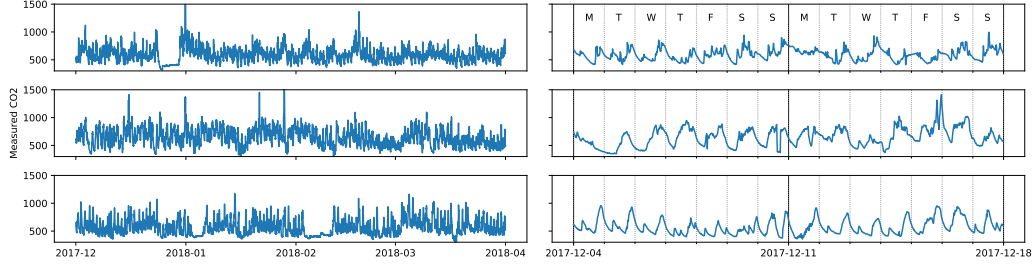


Figure 11: Measured CO₂ air content in the kitchen for three ventilation units. Left: The complete datasets. Right: Closeup of two weeks for each corresponding dataset. A day/night pattern is somewhat discernible, but unlike the Taxi dataset, a weekday/weekend pattern is much less obvious.

480 a typical use case wherein a data scientist has to explore data for which little
481 to nothing is known.

482 We calculated the CMP using the z-normalized Euclidean distance, using
483 a subsequence length of 3 hours and specifying contexts ranging from 06:00
484 until (including) 08:00 in the morning. The results are visualized in Figure 12.
485 We see that all three units display very different morning behavior. The first
486 unit displays a pattern that closely resembles the Taxi dataset, with distinct
487 behavior for weekdays, weekends and holidays. It most likely belongs to a
488 family household with regular school and working hours. The second unit
489 shows no clear patterns, though we can see a change near the end of the
490 dataset. The last unit shows a pattern at the start of the dataset, which
491 changes starting January. While we have no explanation for the behavior in
492 these units, the patterns are still interesting to discover and could prove useful
493 for experts. In parallel, we calculated other CMPs for noon and evening,
494 but do not list them in this paper due to size constraints and refer to the
495 accompanying sources for more details [25].

496 5.4. Ventilation Dataset: Anomaly Detection

497 After exploring the data, we continue here with the dataset for the first
498 unit. We choose this dataset as it shows most similarity to our expectations
499 of a regular household and should therefore be easier to interpret. Similar
500 to the Taxi dataset, we split the CMP into contexts linked to weekdays
501 and weekends. Since the weekday mornings are very similar, the results are
502 quite similar to those of the Taxi dataset and we refer the reader to the
503 supplementary material for more detailed results. Instead, we will focus on

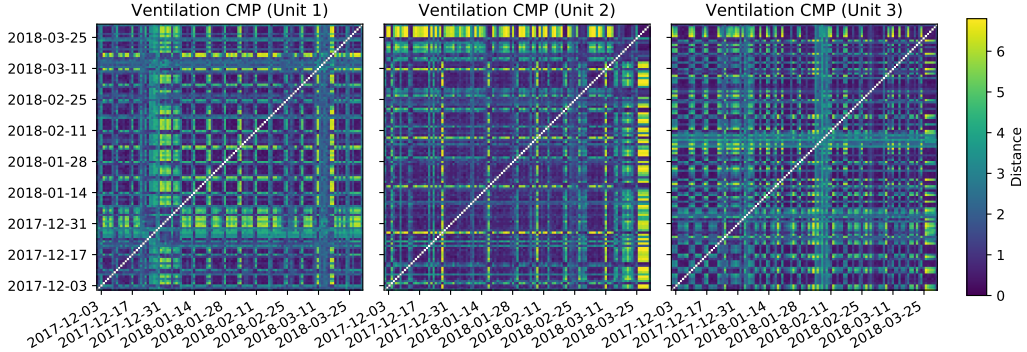


Figure 12: CMP calculated on the morning behavior of three kitchens. The first unit displays a weekday/weekend periodic pattern similar to the Taxi dataset, as well as different behavior around the holiday period. The second unit shows no clear pattern, indicating most mornings have a similar regime. The third unit shows a somewhat periodic pattern that does not match with weekdays/weekends.

504 the more challenging weekend behavior in this section.

505 The weekend measurements do not only have a wider range of behavioral
 506 patterns, but the start time of these patterns also varies from day to day.
 507 Using the CMP calculated on the morning contexts from the previous sec-
 508 tion, we created a smaller CMP only containing weekend days. Unlike the
 509 Taxi dataset, we did not split up Saturdays and Sundays, since there was
 510 no distinctive pattern visible for these days in the CMP data visualization.
 511 Using the Elbow method, we determined the presence of six anomalies.

512 Due to the wide variation of the patterns in both values and time, it
 513 becomes harder to visualize the anomalies in an intuitive way. One useful
 514 approach is a matching table, of which an extract is shown in Figure 13
 515 (the complete figure is available in the source files [25]). Every row of the
 516 table corresponds to a single weekend day (one row in the CMP). This day
 517 is shown in the first column with the morning context highlighted. The
 518 remaining columns show the matches with other weekend days, ordered from
 519 best match to worst match. Rather than showing all matches, we simply
 520 select the matches on all three quartiles, as well as the best and worst match.
 521 Note that each match corresponds to one single value listed in the CMP.

522 When inspecting the contents of the matching table, we see that the
 523 mornings classified as normal have many good matches, only showing mi-
 524 nor differences in the third quartile match. The matches for the anomalous
 525 mornings already show this level of difference in the first quartile, showing

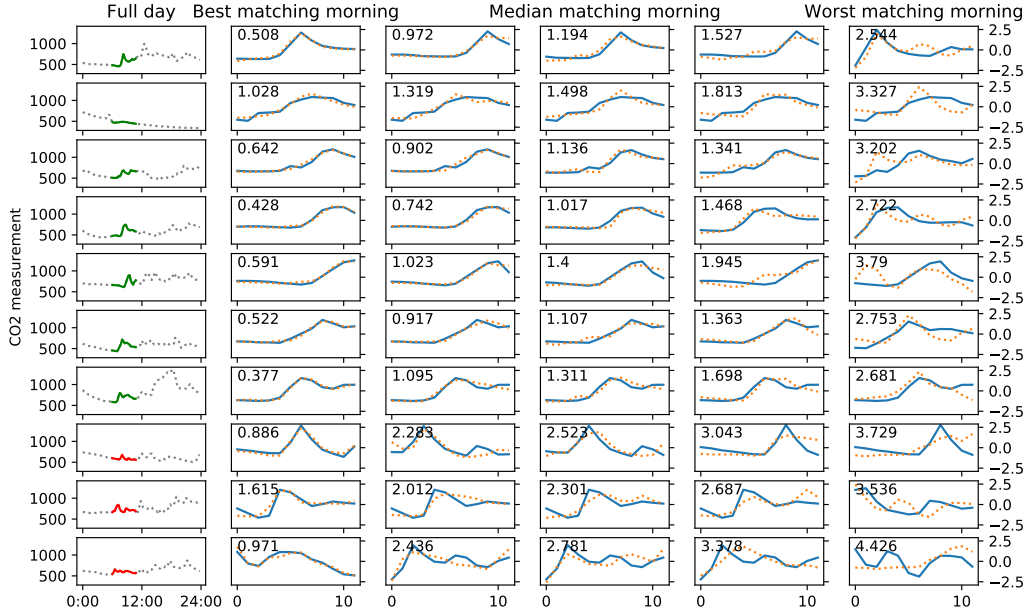


Figure 13: Matching table for subset of weekend days for ventilation unit 1. Each row corresponds to one weekend day, which is displayed in the first column with the morning context (including the window length) highlighted. The first seven rows display days classified as regular (green), the last three show anomalous days (red). The columns show the matching of the morning context (blue) with other morning contexts (dotted orange, one per column). Note that the matching uses subsequences of the context: each blue fragment is a three hour subsequence of the five hour long green/red fragment. For each match, the z-normalized Euclidean distance is displayed in the top left.

that they are in fact uncommon behavior for a weekend morning. This is quantified in the distances listed in Figure 13: the distances of the first quartile match of anomalies are already higher than those of the third quartile of the normal days. Going further into detail, we see that the normal mornings share a common pattern of a plateau followed by a smooth bump and a second, higher plateau. We suspect this pattern is caused by someone waking up, having breakfast in the kitchen and going to an adjacent room. The mornings marked as anomalous show subtly different patterns. The first lacks the second plateau, the second has an earlier start (causing the first plateau to fall outside the context) and also lacks the higher plateau, the third anomaly lacks the distinct high bump at the start. Note that the second normal morning should probably be classified as anomalous. But even though the first spike occurs before the context, the z-normalisation enables

539 a good match between the subtle second bump with the bumps of other
540 days. This again demonstrates the need to finetune the anomaly detection
541 algorithm to the needs of the user.

542 When looking at the matches in detail, we see how the blue subsequences
543 are not exactly the same for each match. Indeed, the contexts used to produce
544 the CMP allow a time shift: the three hour long subsequence should start
545 between 06:00 and 08:00. As we can see, this flexibility allows us to recognize
546 similar behavioral patterns, despite them not being aligned in time. This
547 flexibility comes at the cost of the user having to define the contexts, often
548 having to rely on expert knowledge of the underlying process. In this case,
549 we relied on our personal experience about kitchen usage patterns to define
550 the contexts.

551 5.5. Summary

552 We conclude this section by reiterating our claim that anomaly detection
553 is an inherent subjective topic and difficult to validate. Only when knowing
554 what a user defines as anomalous, can the proper technique be chosen and
555 tried. In this section, we defined normal behavior as behavior that closely
556 matches the majority of the data, and found the CMP to be a suitable
557 technique to detect outliers. We found 18 anomalies for the Taxi dataset,
558 which is more than the five listed as ground truth, and could provide a
559 straightforward explanation for all but one. In the ventilation dataset, we
560 found six anomalies but had no way to validate them independent of the
561 data.

562 One advantage of the CMP over the Matrix Profile for anomaly detection
563 is that the CMP does not depend on the uniqueness of anomalies (it does not
564 simply find discords), but rather on the *the expectations of the user regarding*
565 *normal behavior*. These expectations correspond to the CMP contexts and
566 can be based on the insights retrieved using the CMP for data visualization.
567 As part of the SDM framework, the CMP can be calculated using any dis-
568 tance measure and calculated in parallel with other techniques such as the
569 Matrix Profile.

570 6. Conclusion

571 In this paper we introduced the Series Distance Matrix framework (SDM),
572 a generalisation of the original approach used to calculate the Matrix Profile.
573 The SDM framework splits the generation and consumption of the all-pair

574 subsequence distances, putting the focus on the distance matrix itself. This
575 allows for easier and more flexible experiments by freely combining compo-
576 nents and eliminates the need to re-implement algorithms to combine tech-
577 niques in an efficient way. The extensions of the Matrix Profile can be fitted
578 in this framework as (part of) a SDM-generator or SDM-consumer. Further-
579 more, we suspect new techniques will be discovered by further studying the
580 properties of the distance matrix in future work.

581 We introduced one additional SDM-consumer, namely the Contextual
582 Matrix Profile (CMP). The CMP processes rectangular areas of the distance
583 matrix, compared to the Matrix Profile processing columns. As a result, the
584 CMP is able to compare a range of subsequences against many other ranges,
585 rather than only tracking the best match.

586 We proved the utility of the CMP for two use cases. When used for data
587 visualization, the CMP was able to reveal repetitive and deviating patterns
588 in the data, making it an ideal first step for data exploration, especially for
589 data containing repetitive patterns. When used for anomaly detection, we
590 defined contexts based on our expectations of the data and were able to find
591 anomalies in the contexts not matching those expectations. Unlike the Ma-
592 trix Profile, the CMP is able to detect anomalies that are not discords. Both
593 cases were demonstrated on the New York Taxi dataset and a proprietary
594 ventilation metric dataset. In the former, we were able to reasonably explain
595 all patterns and anomalies. In the latter, we showed the visual difference
596 between different ventilation units and relied on the time shift capability of
597 the CMP to discover anomalous mornings.

598 As part of this publication, we have released a Python implementation of
599 the SDM framework, already comprising implementations for a substantial
600 set of related work. Furthermore, the source code for all use case related
601 processing has been made available online [25].

602 Acknowledgements

603 This research is part of the imec ICON project Dyversify, co-funded by
604 imec, VLAIO, Renson Ventilation NV, Televic Rail & Cumul.io.

605 [1] IoT Analytics, State of the iot 2018: Number of iot devices now at 7b
606 market accelerating, 2018. [https://iot-analytics.com/state-of-](https://iot-analytics.com/state-of-the-iot-update-q1-q2-2018-number-of-iot-devices-now-7b/)
607 [the-iot-update-q1-q2-2018-number-of-iot-devices-now-7b/](https://iot-analytics.com/state-of-the-iot-update-q1-q2-2018-number-of-iot-devices-now-7b/).

- 608 [2] E. Keogh, L. Wei, X. Xi, S.-h. Lee, M. Vlachos, LB - Keogh Sup-
609 ports Exact Indexing of Shapes under Rotation Invariance with Arbi-
610 trary Representations and Distance Measures, in: Proc. of the 32nd
611 Int. Conf. on Very Large Data Bases, VLDB Endowment, Seoul, Korea,
612 2006, pp. 882–893.
- 613 [3] Y. Lei, N. Li, L. Guo, N. Li, T. Yan, J. Lin, Machinery health pro-
614 gnostics: A systematic review from data acquisition to RUL prediction,
615 Mechanical Systems and Signal Processing 104 (2018) 799–834.
- 616 [4] D. Vries, B. van den Akker, E. Vonk, W. de Jong, J. van Summeren,
617 Application of machine learning techniques to predict anomalies in wa-
618 ter supply networks, Water Science and Technology: Water Supply 16
619 (2016) 1528–1535.
- 620 [5] C.-C. M. Yeh, Y. Zhu, L. Ulanova, N. Begum, Y. Ding, H. A. Dau,
621 D. F. Silva, A. Mueen, E. Keogh, Matrix Profile I: All Pairs Similarity
622 Joins for Time Series: A Unifying View That Includes Motifs, Discords
623 and Shapelets, in: 2016 IEEE 16th Int. Conf. on Data Mining (ICDM),
624 IEEE, 2016, pp. 1317–1322.
- 625 [6] Y. Zhu, Z. Zimmerman, N. S. Senobari, C.-C. M. Yeh, G. Funning,
626 P. Brisk, E. Keogh, Matrix Profile II : Exploiting a Novel Algorithm
627 and GPUs to Break the One Hundred Million Barrier for Time Series
628 Motifs and Joins, 2016 IEEE 16th Int. Conf. on Data Mining (ICDM)
629 (2016) 739–748.
- 630 [7] C.-C. M. Yeh, H. Van Herle, E. Keogh, Matrix profile III: The matrix
631 profile allows visualization of salient subsequences in massive time series,
632 Proceedings - IEEE Int. Conf. on Data Mining, ICDM (2017) 579–588.
- 633 [8] C.-C. M. Yeh, N. Kavantzas, E. Keogh, Matrix profile IV: Using Weakly
634 Labeled Time Series to Predict Outcomes, Proc. of the VLDB Endow-
635 ment 10 (2017) 1802–1812.
- 636 [9] H. A. Dau, E. Keogh, Matrix Profile V: A Generic Technique to Incor-
637 porate Domain Knowledge into Motif Discovery, in: Proc. of the 23rd
638 ACM SIGKDD Int. Conf. on Knowledge Discovery and Data Mining -
639 KDD '17, ACM Press, New York, New York, USA, 2017, pp. 125–134.

- 640 [10] C.-C. M. Yeh, N. Kavantzas, E. Keogh, Matrix Profile VI: Meaningful
641 Multidimensional Motif Discovery, in: 2017 IEEE Int. Conf. on Data
642 Mining (ICDM), IEEE, 2017, pp. 565–574.
- 643 [11] Y. Zhu, M. Imamura, D. Nikovski, E. Keogh, Matrix Profile VII: Time
644 Series Chains: A New Primitive for Time Series Data Mining, in: 2017
645 IEEE Int. Conf. on Data Mining (ICDM), IEEE, 2017, pp. 695–704.
- 646 [12] S. Gharghabi, Y. Ding, C.-C. M. Yeh, K. Kamgar, L. Ulanova, E. Keogh,
647 Matrix Profile VIII: Domain Agnostic Online Semantic Segmentation
648 at Superhuman Performance Levels, in: 2017 IEEE Int. Conf. on Data
649 Mining (ICDM), IEEE, 2017, pp. 117–126.
- 650 [13] R. Akbarinia, B. Cloez, Efficient Matrix Profile Computation Using Dif-
651 ferent Distance Functions, 2019.
- 652 [14] D. Furtado Silva, G. E. A. P. A. Batista, Elastic Time Series Motifs
653 and Discords, in: 2018 17th IEEE Int. Conf. on Machine Learning and
654 Applications (ICMLA), IEEE, 2018, pp. 237–242.
- 655 [15] D. De Paepe, O. Janssens, S. Van Hoecke, Eliminating Noise in the Ma-
656 trix Profile, in: Proceedings of the 8th Int. Conf. on Pattern Recog-
657 nition Applications and Methods, SCITEPRESS - Science and Technology
658 Publications, 2019, pp. 83–93.
- 659 [16] Y. Zhu, C.-C. M. Yeh, Z. Zimmerman, K. Kamgar, E. Keogh, Matrix
660 Profile XI: SCRIMP++: Time Series Motif Discovery at Interactive
661 Speeds, in: 2018 IEEE Int. Conf. on Data Mining (ICDM), IEEE, 2018,
662 pp. 837–846.
- 663 [17] M. Linardi, Y. Zhu, T. Palpanas, E. Keogh, Matrix Profile X, in: Proc.
664 of the 2018 Int. Conf. on Management of Data - SIGMOD ’18, ACM
665 Press, 2018, pp. 1053–1066.
- 666 [18] E. Keogh, S. Kasetty, On the need for time series data mining bench-
667 marks, Proc. of the 8th ACM SIGKDD Int. Conf. on Knowledge dis-
668 covery and data mining - KDD ’02 (2002) 102.
- 669 [19] A. Mueen, Y. Zhu, M. Yeh, K. Kamgar, K. Viswanathan, C. Gupta,
670 E. Keogh, The fastest similarity search algorithm for time series

- 671 subsequences under euclidean distance, 2017. <http://www.cs.unm.edu/~mueen/FastestSimilaritySearch.html>.
- 672
- 673 [20] D. De Paepe, D. Nieves Avendano, S. Van Hoecke, Implications of Z-
674 Normalization in the Matrix Profile, 2019.
- 675 [21] Y. Zhu, A. Mueen, E. Keogh, Admissible Time Series Motif Discovery
676 with Missing Data (2018).
- 677 [22] D. F. Silva, C.-c. M. Yeh, Y. Zhu, G. E. A. P. A. Batista, E. Keogh,
678 Fast Similarity Matrix Profile for Music Analysis and Exploration, IEEE
679 Transactions on Multimedia 21 (2019) 29–38.
- 680 [23] S. Imani, F. Madrid, W. Ding, S. Crouter, E. Keogh, Matrix Profile XIII:
681 Time Series Snippets: A New Primitive for Time Series Data Mining,
682 in: 2018 IEEE Int. Conf. on Big Knowledge (ICBK), IEEE, 2018, pp.
683 382–389.
- 684 [24] S. Gharghabi, S. Imani, A. Bagnall, A. Darvishzadeh, E. Keogh, Matrix
685 Profile XII: MPdist: A Novel Time Series Distance Measure to Allow
686 Data Mining in More Challenging Scenarios, in: 2018 IEEE Int. Conf.
687 on Data Mining (ICDM), IEEE, 2018, pp. 965–970.
- 688 [25] Source code for our experiments, 2019. <https://sites.google.com/view/generalizing-matrix-profile>.
- 689
- 690 [26] A. Lavin, S. Ahmad, Evaluating Real-Time Anomaly Detection Algo-
691 rithms – The Numenta Anomaly Benchmark, in: 2015 IEEE 14th Int.
692 Conf. on Machine Learning and Applications, IEEE, 2015, pp. 38–44.
- 693 [27] N. Kumar, V. N. Lolla, E. Keogh, S. Lonardi, C. A. Ratanamahatana,
694 L. Wei, Time-series Bitmaps: a Practical Visualization Tool for Working
695 with Large Time Series Databases, in: Proc. of the 2005 SIAM Int. Conf.
696 on Data Mining, Society for Industrial and Applied Mathematics, 2005,
697 pp. 531–535.
- 698 [28] V. Chandola, A. Banerjee, V. Kumar, Anomaly detection: A Survey,
699 ACM Computing Surveys 41 (2009) 1–58.
- 700 [29] H. Sivaraks, C. A. Ratanamahatana, Robust and accurate anomaly
701 detection in ECG artifacts using time series motif discovery, Computa-
702 tional and Mathematical Methods in Medicine 2015 (2015).